

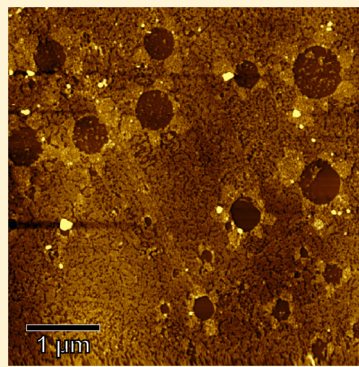
Covering Surface Nanobubbles with a NaCl Nanoblanket

Robin P. Berkelaar,^{*,†,‡,§} Harold J. W. Zandvliet,^{*,‡} and Detlef Lohse^{*,§}

[†]Materials Innovation Institute (M2i), 2628 CD Delft, The Netherlands

[‡]Physics of Interfaces and Nanomaterials, [§]Physics of Fluids, MESA+ Institute for Nanotechnology, University of Twente, P.O. Box 217, 7500 AE Enschede, The Netherlands

ABSTRACT: By letting a NaCl aqueous solution of low (0.01 M) concentration evaporate on a highly oriented pyrolytic graphite (HOPG) surface, it is possible to form a thin film of salt. However, pre-existing surface nanobubbles prevent the homogeneous coverage of the surface with the salt, keeping the footprint areas on the substrate pristine. Comparing the surface nanobubbles in the salt solution with their associated footprint after drying, provides information on the shrinkage of nanobubbles during the hours-long process of drying the liquid film. At a slightly higher NaCl concentration and thus salt layer thickness, the nanobubbles are covered with a thin blanket of salt. Once the liquid film has evaporated until a water film remains that is smaller than the height of the nanobubbles, the blanket of salt cracks and unfolds into a flower-like pattern of salt flakes that is located at the rim of the nanobubble footprint. The formation of a blanket of salt covering the nanobubbles is likely to considerably or even completely block the gas out-flux from the nanobubble, partially stabilizing the nanobubbles against dissolution.



INTRODUCTION

In 1994, Parker et al.¹ measured discrete steps in the force-distance curve between two hydrophobic glass surfaces. This was the first indication of the existence of submicrometer bubbles at solid–liquid interfaces, the so-called surface nanobubbles.^{2,3} The first real-space images of nanobubbles were recorded a few years later using an atomic force microscope (AFM) by Ishida et al.⁴ and Lou et al.⁵ The fact that these nanobubbles were actually measured over a time scale of several hours up to days,^{6,7} though classical theory dictates that nanobubbles should dissolve in the order of microseconds,⁸ started the growth of the nanobubble field. Several different theories have since then been put forward explaining the unusual stability. One of the first conjectures was that the nanobubbles had to be covered by a dense contamination layer, effectively blocking the diffusion of gas.^{9–12} In contrast, experiments using surfactants had no effect on the lifetime of nanobubbles.¹³ According to another theory introduced by Brenner and Lohse,¹⁴ the nanobubbles are in a dynamic equilibrium, gas leaving the bubble is compensated by gas re-entering at the three-phase contact line. However, it is unclear what the underlying mechanism is that drives gas recirculation for such a prolonged time.¹⁵ Alas, the energy source governing this recirculation remains elusive. Just recently an attractive theory was introduced by Weijs et al.¹⁶ Assuming nanobubbles are pinned, which is experimentally observed by Zhang et al.,⁷ together with the upward diffusion of gas toward the atmosphere, results in dissolution times much slower than what is predicted for nanosized bubbles in the bulk. The behavior of nanobubbles and the validity of the theories described above have been tested by changing a variety of parameters such as temperature,^{17–19} gas type,²⁰ substrate,^{5,17,21–24} and pH.^{25,26} Also a variety of chemicals have

been added to the liquid like proteins,^{27,28} salts,^{26,25} and particles.²⁹

Direct investigation of the geometry of individual nanobubbles in thin liquid layers of only several micrometers thick is impossible by AFM, due to the adverse effect of the capillary forces on the AFM tip. In this work, we use NaCl in aqueous solution to study the geometry of nanobubbles *in situ* in wet conditions as well as *ex situ* in a dried environment. One of the properties of NaCl is the possibility to grow thin carpet-like layers of salt over stepped surfaces.³⁰ Using the fact that a NaCl solution starts to crystallize at a critical concentration, together with low NaCl concentrations, makes it possible to imprint the nanobubbles just before complete drying. The imprint provides information on the geometry of individual nanobubbles without the adverse effect of capillary forces on the AFM tip. Zhang et al.²⁵ have shown that nanobubbles are insensitive to the addition of salt once the nanobubbles have formed. This, together with the carpet-like growth and the high solubility, makes NaCl a good material to study the effect of thin liquid films on the geometry of individual nanobubbles with high resolution.

EXPERIMENTAL DETAILS

In the case of highly oriented pyrolytic graphite (HOPG), it is easy to achieve nucleation of nanobubbles, simply by depositing a drop of Millipore water onto the surface. The Millipore water in this study was prepared using a Simplicity 185 system (Millipore). The substrate was ZYA grade HOPG (MikroMasch), freshly cleaved prior to each experiment. The HOPG sample was clamped in a Teflon liquid cell,

Received: July 2, 2013

Revised: August 9, 2013

Published: August 12, 2013

and a drop of Millipore water ($\sim 0.1 \text{ cm}^3$) was deposited on the surface using an unused syringe (Discardit, BD) and needle (Microlance, BD). The salt solution was prepared by dissolving NaCl (Suprapur 99.99% purity, Merck) in Millipore water to a concentration of 0.02 M. Approximately 0.1 cm^3 solution was injected in the Millipore droplet on the HOPG surface, finally resulting in a concentration of 0.01 M of NaCl and a total volume of $\sim 0.2 \text{ cm}^3$. This two step process was performed to ensure that the salt solution had no effect on the nucleation of the nanobubbles. The Teflon liquid cell was then placed within an Agilent 5100 AFM. Both the Teflon liquid cell and AFM nose-cone were rinsed thoroughly with ethanol (Emsure 96% purity, Merck) and dried in a N_2 gas flow before the experiment. The immersed surface covered with nanobubbles was imaged by the AFM operated in intermittent contact mode. Next, the liquid cell was removed from the AFM and left to dry in a temperature (21°C) and humidity (40%) controlled environment. Evaporation time was controlled by covering the liquid cell with a sheet of perforated Parafilm, the amount of perforation effectively varies the area of the liquid cell exposed to the environment, which resulted in evaporation times of approximately 11–12 h. Finally, after all the water had evaporated from the HOPG substrate, it was placed back into the AFM and the now dry surface was imaged. The unique step-edge fingerprint of HOPG in combination with an optical microscope made it possible to scan the exact same surface area at both wet and dry conditions. The AFM cantilevers were Al-back-coated NSC36c Si_3N_4 probes obtained from MikroMasch with a nominal spring-constant of 0.6 N/m, resonance frequency of $\omega_0 = 65 \text{ kHz}$, and tip radius of 8 nm. The NSC36c cantilever was used to scan the surface in wet conditions as well as after drying. The set-point was kept as high as possible (~95%) and the amplitude was between 20 and 30 nm in order to minimize the deformation of the nanobubbles by the tip. The resonance frequency is much lower in water and amounts $\omega_{0,w} = 34 \text{ kHz}$.

RESULTS AND DISCUSSION

A typical AFM image of nanobubbles on HOPG in a 0.01 M NaCl solution is shown in Figure 1A. The vertical lines seen in

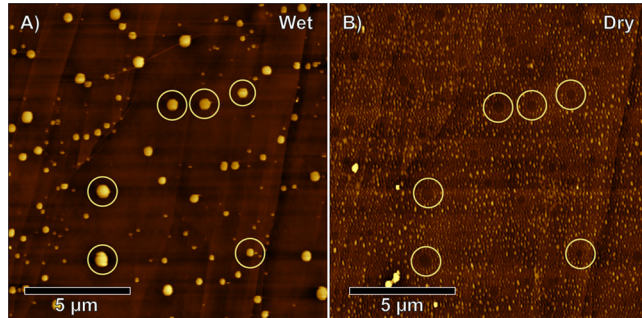


Figure 1. (A) Nanobubbles on HOPG in a 0.01 M NaCl solution. Some nanobubbles are encircled to guide the eye. After injecting a NaCl solution, the surface is dried and the exact same area is imaged again. The dry HOPG surface is now covered with NaCl crystals, except for the positions nanobubbles had been present (B). The circles in both images (A,B) show a direct relation between nanobubble and the NaCl-deprived footprint. Evaporation time was approximately 11 h.

the image are step-edges of the HOPG substrate. Many nanobubbles have nucleated on the surface (a few are encircled to guide the eye) with a broad distribution of sizes. The surface is imaged again after all the water had evaporated, see Figure 1B. The step-edges in Figure 1A,B clearly show that the exact same area is scanned under both wet and dry conditions. During evaporation, the concentration of NaCl in the droplet increases until it reaches the saturation concentration of 360 g/

L. After that the ongoing evaporation leads to the nucleation of NaCl crystals. Heterogeneous nucleation³¹ is preferred over homogeneous nucleation³² due to the lower effective surface energy needed for the former. That is why NaCl crystals start to nucleate at the solid–liquid and gas–liquid interfaces, rather than homogeneous nucleation in the bulk. The dry surface is finally covered with small NaCl crystals of approximately 3 nm in size, which nucleated at the surface. Interestingly, comparing the position of the nanobubbles with the same position on the dry substrate (circles highlight the same position on the wet as well as on the dry surface) shows that no NaCl crystals have nucleated at the positions of the nanobubbles. The reason is that nanobubbles locally prevent the NaCl solution from wetting the HOPG and thus no nucleation of NaCl crystals can occur at these locations. In one of the experiments the wet surface was continuously scanned in order to observe the onset of NaCl crystal nucleation. However, no nucleation was observed up to the point that capillary forces of the thin liquid film were affecting the cantilever and the measurement had to be stopped. Nonetheless, it is possible to estimate the onset of NaCl crystallization using the fact that the solubility of NaCl in water is 360 g/L. Approximating the drop by a cylindrical shape and assuming that the droplet remains pinned in reality the contact-line of the droplet decreases in a stick-slip motion), we can calculate the liquid thickness at which the concentration is equal to the solubility level. This thickness is in the order of micrometers. Due to stick-slip of the droplet this value will in reality be slightly larger but still in the same order of magnitude. Even so, it shows that the nanobubbles have to exist at least till the water film has decreased to the critical thickness of several μm in order to prevent the solution from wetting the HOPG.

The ease of scanning the same area in both wet and dry conditions on HOPG, as well as the onset of NaCl crystallization at very thin liquid films opens up the possibility to compare one-to-one what happens to the position and radius of the nanobubbles at the end of their lifetime. In Figure 2, the line-profile through the center of a nanobubble is shown (dashed blue line) together with the line-profile of the associated footprint after drying the surface (red line). The footprint has an upstanding rim at its perimeter, probably due

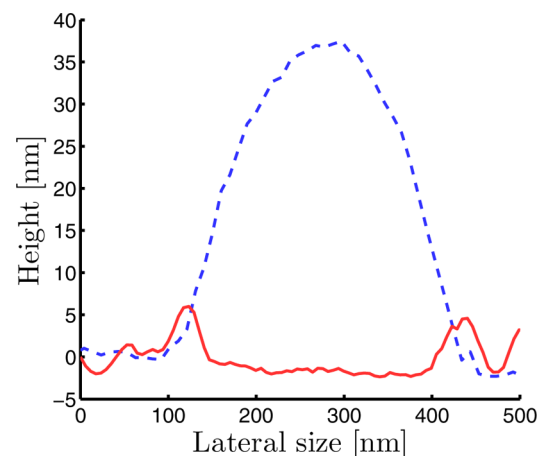


Figure 2. A line profile of a nanobubble on HOPG prior to the injection of NaCl (dashed blue line). The associated footprint after injecting a NaCl solution and drying the surface (red continuous line). Comparison of both line profiles shows a slightly smaller footprint radius compared to the nanobubble radius.

to the heterogeneous gas–liquid interface of the bubble that supports the growth of NaCl crystals at the HOPG surface. This results in slightly larger crystal sizes at the three-phase contact line. Even more intriguing is that the radius of the footprint compared to that of the nanobubble is slightly smaller.

The obvious question that arises is the following: did the nanobubbles slightly shrink? In order to answer this question, the radii of a few hundred nanobubbles and their associated footprints were analyzed. The experiments are very reproducible; the data in Figure 3 are the result of four distinct

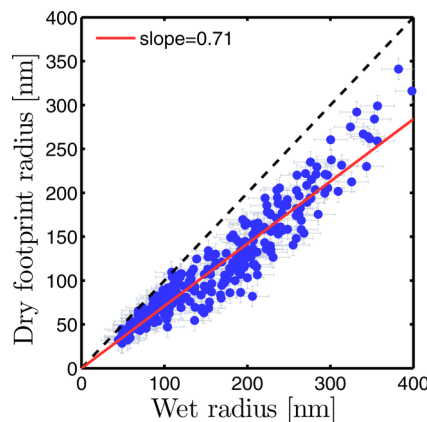


Figure 3. Dry footprint radius as a function of wet nanobubble radius, both corrected for convolution with the AFM tip. The general trend shows a slightly smaller dry footprint compared to the associated nanobubble radius. Fitting the data with a linear line using the least-squares method results in a ratio of approximately 0.71 (red continuous line). The black dashed line has a ratio of 1:1 as comparison.

experimental runs with freshly cleaved HOPG and newly prepared NaCl solution. More experiments resulted in a successful imprint of nanobubbles in a layer of salt, however, it was not possible for every experiment to make a one-to-one comparison between dry and wet conditions. The dry footprint radius is plotted as a function of the nanobubble radius in Figure 3. The radii of the nanobubbles have been corrected for tip convolution using the method of Kameda et al.³³ The effect of the AFM tip on the apparent radii of the nanobubbles can be neglected when scanning at high set-points (>95%).⁴⁰ The general trend reveals a slightly smaller footprint radius compared to the associated nanobubble radius. A first order fit, using the least-squares method, results in a slope of approximately 0.71. The fact that this ratio holds for small as well as larger nanobubbles excludes the possible decrease in footprint ratio due to the inward growth of NaCl crystals at the nanobubble perimeter. The velocity of this inward growth should be radially independent, which results in a fixed offset between nanobubble and footprint radii, not in a change of their ratio. We therefore think that the smaller footprint radius is evidence for a small shrinkage of the nanobubbles. Larger nanobubbles appear to shrink a bit more than smaller nanobubbles. Although the liquid film at the moment of the salt nucleation was of the order of micrometers, the shrinkage of nanobubbles seems to be rather small and it appears that the thin liquid film has a negligible effect on the dissolution of the nanobubble. The decrease in radius also shows that the nanobubbles are not completely pinned; at least the contact-

line of the nanobubbles undergoes stick–slip motion while shrinking.

Also on a larger length scale there is no complete pinning. during the evaporation of the NaCl solution, the droplet contact line undergoes stick–slip jumps, resulting in an increased NaCl deposition near the center. Imaging close to the edge toward the center of the NaCl deposition results in different footprints due to the increasing salt thickness. Figure 4A shows a homogeneous distribution of NaCl crystals

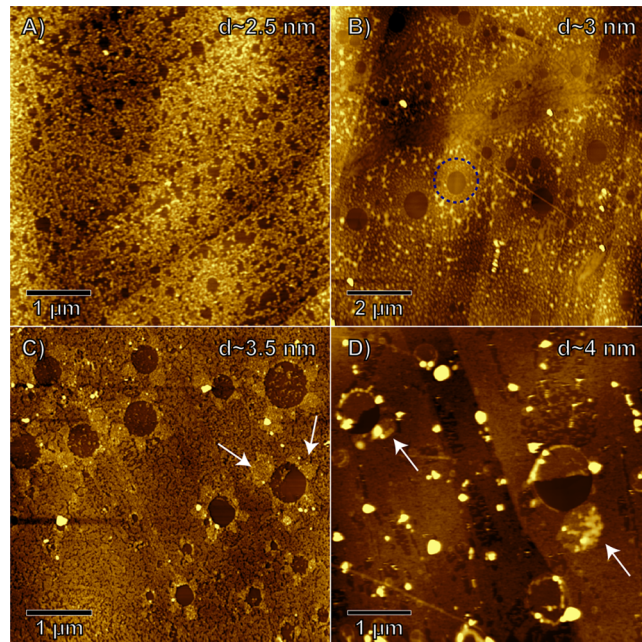


Figure 4. The observed footprints after drying the NaCl solution changes with increasing NaCl thickness. A ~ 2.5 nm thick NaCl layer displays a surface homogeneously covered with NaCl crystals, except for small areas of pristine HOPG, at positions where nanobubbles had been present (A). Larger NaCl crystals form when the NaCl layer thickness is increased to ~ 3 nm (B). These larger crystals, however, do not form near a nanobubble. A depletion zone of NaCl crystals is found to exist around the footprints (blue dashed circle). At a thickness of ~ 3.5 nm flower-like layers of NaCl crystals (pointed out by white arrows) exist around the footprints (C). In (D) the footprints end up partially filled with a NaCl layer with the remainder lying around the footprint (pointed out by white arrows), the NaCl thickness in this case is ~ 4 nm. Some footprints are even completely filled with salt and the footprints can only be observed from the fact they have an upstanding rim.

(average height ~ 2.5 nm) with footprints and pristine HOPG regions due to the protection from the NaCl solution by nanobubbles. At a slightly higher salt thickness (average height ~ 3 nm) the footprints still comprise of pristine HOPG (within the limits of the AFM resolution), see Figure 4B. However, the distribution of the NaCl crystal sizes is less monodisperse. Besides the relative large coverage of small crystals some of the crystals have grown to a slightly larger size. Interestingly, near the footprints there is a region where no large crystals are found, that is, NaCl depletion zones exist (blue dashed line).

Zooming in on one of these depletion zones reveals more details (Figure 5A). The unmasked disk is the area over which the average height as a function of radius is calculated, with the footprint as center, see Figure 5B. The first peak in this graph (highlighted with a red dashed line) is the rim around the

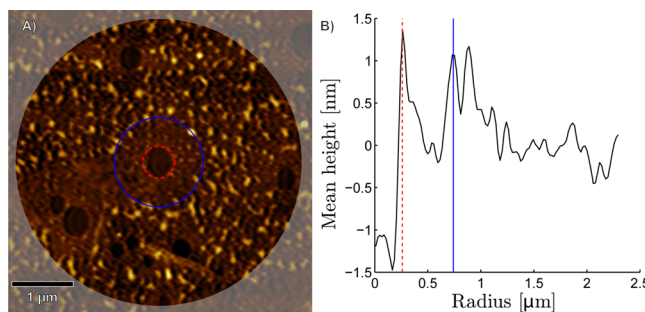


Figure 5. A zoom in on one of the footprints from Figure 4 in a NaCl layer of ~3 nm thick (A). Starting with the center of the footprint the mean radial height is shown (B). The first peak represents an upstanding rim around the footprint (red dashed line). The second peak shows the starting radius at which larger NaCl are observed (blue line). The area between both lines is the depletion zone. The amount of NaCl present in this area is lower compared to the average.

footprint, clearly showing a pile up of salt. Next is a region with less salt, which ends at a second peak (highlighted with a blue line). This second peak shows the perimeter of the NaCl depletion zone. Comparison with measurements at the same position in wet conditions shows that the nanobubble and footprint radii are of similar sizes. This excludes the possibility that the depletion zones were formed by the shrinkage of nanobubbles. Although most of the footprints are in the center of this depletion zone, this is not always the case. This makes us believe that the depletion zone does not emerge from a convection effect, caused by Marangoni stresses due to NaCl concentration differences. Convective effects would leave symmetrical depletion zones with the footprint in the center and the symmetry only broken by the proximity of other nanobubbles. However, some footprints are observed at the edge of the depletion zone without nanobubbles in the proximity. The logical explanation for the depletion zone is the presence of a densely adsorbed gas layer, also referred to as a micropancake.^{34–38} Nanobubbles are often observed on top of micropancakes. The location can be at any position, either in the center or at the edges of the micropancake. The presence of such a densely adsorbed gas layer between the HOPG surface and the salt solution will inhibit the formation of NaCl crystals, resulting in a depletion zone of salt wherever a micropancake is present. The densely adsorbed gas layer is most probably a thin epitaxial layer on the underlying HOPG substrate.³⁸ This layer will be a more suitable template for NaCl crystal nucleation than a purely gaseous, that is, nanobubble, interface.

At an average salt thickness of ~3.5 nm, a completely different salt distribution is observed, see Figure 4C. The salt crystals on the surface are densely packed, appearing almost like a closed thin salt film. In this salt layer, the footprints of the nanobubbles are easily observed. However, compared to the pristine HOPG footprints in areas with less salt, these footprints still contain a few NaCl crystals. Most interesting are the flower-like structures around the footprints. With the increase of NaCl concentration, nucleation of crystals not only occurs at the HOPG surface, but also on the gas–liquid interface of the nanobubble. The nanobubbles are covered in a thin layer of densely packed NaCl crystals, similar to the salt layer on the HOPG. This layer of salt breaks and folds open around the footprint, giving a flower-like pattern. During cracking of this blanket of salt, some crystals will detach completely and fall onto the footprint, which is the cause of the

less pristine footprint. The structural strength of the salt layer increases with increasing thickness and the number of cracks goes down to the point that the blanket of salt does not break anymore at all, see Figure 4D. Although even the complete footprint can be filled with the blanket of salt, the original position where the nanobubble had been is still visible due to the salt rim that formed around the three-phase contact line of the nanobubble. It is clear from image 4D that the blanket of salt on the larger nanobubbles breaks into two parts, half of the blanket falls onto the footprint, while the other half folds away and lies at the edge of the footprint. For the smaller nanobubbles, the blanket of salt does not break and a continuous layer of salt fills the footprints. The large white features are NaCl crystals probably formed in bulk solution. The crystal size is much larger compared to the crystals that nucleated on the HOPG surface due to the 3D growth of these crystals, while on the HOPG the 3D symmetry is broken by the surface, resulting in slower growth and thus smaller crystal sizes.

Using the leaflike patterns around the footprints the shape of the nanobubble at the moment the layer of salt broke can be reconstructed. Nanobubbles have a spherical cap geometry, which can be reconstructed using the footprint radius and contact angle. To deduce the contact angle, the spherical cap surface area is plotted against the footprint area for a number of nanobubbles, see Figure 6B. A typical flower-like pattern is

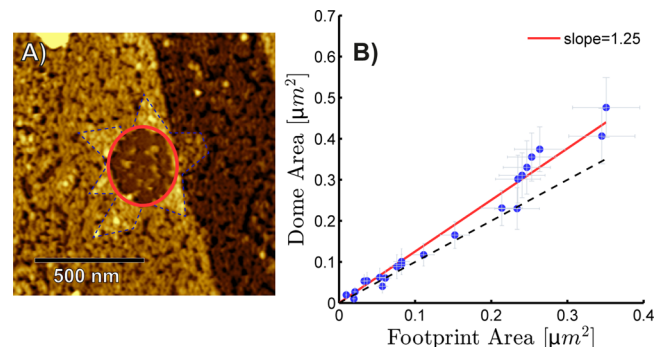


Figure 6. A typical footprint (red line) with the leaflike pattern (blue dashed line) around it is shown (A). The area of the leaflike layers around a footprint is plotted as a function of the footprint area (B). Fitting the data with a linear line using the least-squares method results in a ratio of approximately 1.25 (red continuous line). The difference in area can be easily explained by a NaCl layer that formed over the nanobubble and unfolded into the leaflike layers around the footprint. Thus the combined area of the leaflike salt layers is actually the area of a spherical cap.

shown in Figure 6A. The spherical cap area is the sum of all the salt layers around the footprint that were part of the blanket of salt covering the nanobubble, delineated by the blue dashed line. The reconstructed spherical cap area is larger than the measured footprint area. This is additional evidence that the salt layers were part of a 3D structure before unfolding. Assuming the nanobubbles have a spherical cap shape, the contact angle θ , can be deduced from the ratio a between the spherical cap area and the footprint area

$$\cos(\theta) = 1 - \frac{2(a - 1)}{a} \quad (1)$$

Fitting the data in Figure 6B with the least-squares method gives a slope of 1.25. Using eq 1, results in a contact angle of 127° (liquid side). This number is slightly larger than what is

normally obtained for nanobubbles using AFM. However, it is not far off compared to the value of 135° extrapolated by Walzciek et al.³⁹ and the 119° measured by Borkent et al.⁴⁰ It shows that at the moment the salt film tore apart the nanobubble still had the height and contact angle which is typical for nanobubbles.

The question that remains is: how does the salt film on the nanobubble break open and form such a nice symmetrical pattern? As the water layer becomes thinner van der Waals forces start to have an effect on the stability and the thin film will breakup in small droplets of water.⁴¹ Some water will remain around the nanobubble due to pinning and the capillary forces will pull radially outward on the thin salt film, see Figure 7. If thin-film rupture alone would play a role here, the whole

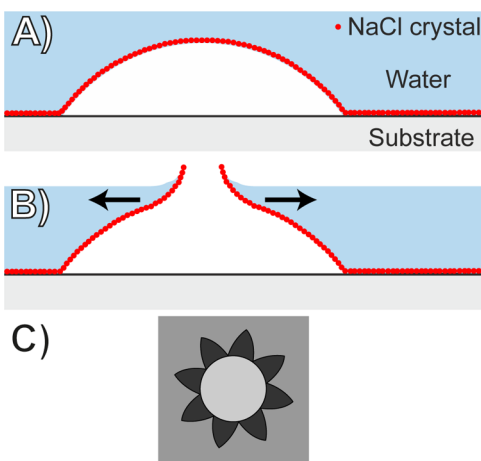


Figure 7. Sketch of the suggested mechanism: a layer of NaCl crystals forms at the nanobubble interface when the NaCl concentration is sufficiently high (A). Because of evaporation the water layer decreases and the liquid–gas interface will touch the nanobubble at a certain point. The capillary forces will break the blanket of salt covering the nanobubble and pull it radially outward (B). Because of the pulling of capillary forces in radial outward direction a leaflike pattern of NaCl layers will be deposited around the nanobubble footprint (C).

event would be highly energetic and the NaCl crystals would be scattered around the footprint. However, the blanket of salt has apparently enough structural strength to oppose the pulling of the surface tension. The thin salt film does crack and is folded outward due to the surface tension, much like capillary origami.⁴² A thicker salt layer will oppose the capillary forces more efficiently, resulting in a lower number of breaking directions or even no cracking at all, as seen in Figure 4D. In the case where the blanket of salt is thick enough to oppose the capillary forces, no breaking of the film will occur and the salt film will cover the footprint area of the nanobubble. In Figure 8, the circular footprint area is still visible but there is a square-like pattern in the salt film covering the footprint. The pattern is the result of the build up of strain, the area of the salt film is larger due to the spherical cap geometry compared to the footprint area it is covering. In order to relieve the stress, the thin film starts to wrinkle and forms this very typical square pattern.⁴³

Crystals formed by nucleation in the bulk liquid are usually larger than crystals formed at an interface, such as HOPG-liquid or a gas–liquid interface of a nanobubble. In Figure 9, a dried HOPG surface covered with a salt layer and many large NaCl crystals is shown. The footprints covered with the deflated blanket of salt are still visible, however, many large crystals are

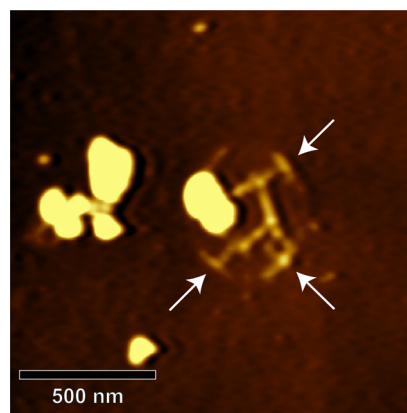


Figure 8. In the case of a NaCl layer with a thickness of 4 nm or larger the capillary forces are not strong enough to break the NaCl layer covering a nanobubble. In this case, the nanobubble just deflates. However, the area of the spherical cap is larger than its footprint area. The surplus of area leads to the formation of wrinkles at the rim of the nanobubble (pointed out by white arrows) as well as a square wrinkle in the center.

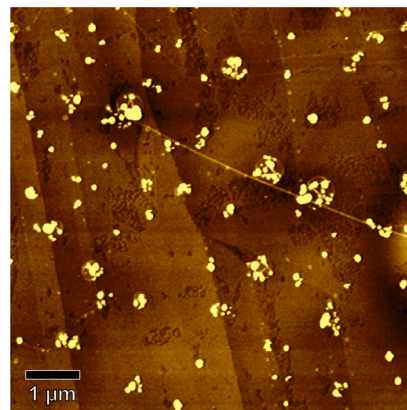


Figure 9. For high concentrations of NaCl, not only is a layer of heterogeneously nucleated salt formed but also homogeneous salt nucleation will occur. These nuclei will form large crystals and have a tendency to adhere to NaCl covered nanobubbles.

lying on the blanket of salt covering the footprint. The nanobubbles exist until the thickness of the liquid layer is of the same order as the height of the nanobubbles, as a result the nanobubbles or the blanket of salt covering the nanobubbles act as preferred adhesion sites for the relatively large NaCl crystals.

CONCLUSION

Evaporating a salt solution of low (0.01 M) concentration results in the formation of a NaCl thin film in the order of a few nanometers. However, footprints of nanobubbles are observed as areas of pristine HOPG. It is clear that nanobubbles are able to prevent the formation of salt crystals on HOPG. Since the crystallization occurs when the liquid film is of the order of micrometers and nanobubble footprints are observed, the nanobubbles are at least stable until the water film has reached the micrometer range. Comparing the nanobubbles with the associated footprints shows a small decrease in nanobubble radius. This suggests nanobubbles are not completely pinned and exhibit stick-slip during shrinkage. For a slightly increased salt concentration, the salt not only nucleates at the HOPG surface, but a thin layer of NaCl crystals also forms at the gas–

liquid interface of the nanobubble. When the water film has evaporated toward a layer thickness of the order of the height of the nanobubbles, capillary forces start pulling radially outward on the blanket of salt covering the nanobubble. If the blanket of salt is sufficiently thick, the capillary forces are not enough to break it and a continuous film will cover the nanobubble footprint. However, as the area of this blanket of salt is larger than the footprint area a wrinkle pattern forms to relieve the resulting stress. Thinner salt films cannot withstand the capillary forces, which results in breaking of the salt film and unfolding into a very distinct flower-like pattern.

Assuming a spherical cap geometry of nanobubbles the shape of the nanobubble can be reconstructed using this flower-like pattern. The reconstruction shows that the contact angle of the nanobubbles is comparable to what is measured in water, even though the water film was reduced to nanometer thickness. The fact that nanobubbles have similar sizes after several hours and even after the water has evaporated to nanometer range shows they are remarkably stable. This observation, together with the formation of a thin salt film limits possible stability theories. Stability by dynamic equilibrium¹⁴ is a very delicate balanced process and the formation of a blanket of salt over the nanobubble would almost certainly disturb the equilibrium. The diffusive stability theory¹⁶ predicts a decrease in nanobubble height over several hours, dependent on the thickness of the liquid film. However, the reconstructed contact angle using the flower-like footprints shows that the nanobubbles have similar heights even after several hours. Of course, the addition of 0.01 M NaCl will lower the gas solubility in the solution, increasing the gas-saturation by approximately 1%. However, the reduction of the liquid film by evaporation down to the order of nanometers will have a significant adverse effect on the stability, as a thinner liquid film would enhance the dissolution of nanobubbles. A viable stability mechanism for nanobubbles in a salty solution would be the complete or partial blockade of gas out-flux by a thin layer around the gas–liquid interface of the nanobubble, in analogy to a pickering type of stabilization seen in emulsions. The fact that a thin NaCl film is found to cover the nanobubbles is in favor of this suggested stability mechanism. Of course, the stability mechanism in an experiment not perturbed by the addition of salt can be of a different kind.

AUTHOR INFORMATION

Corresponding Authors

*E-mail: r.p.berkelaar@utwente.nl

*E-mail: h.j.w.zandvliet@utwente.nl

*E-mail: d.lohse@utwente.nl

Notes

The authors declare no competing financial interest.

ACKNOWLEDGMENTS

This research was carried out under project number M61.3.10403 in the framework of the Research Program of the Materials innovation institute (M2i, www.m2i.nl). We would like to thank Stefan Kooij, Erik Dietrich, Joost Weijs, and in particular James Seddon for many fruitful discussions.

REFERENCES

- (1) Parker, J. L.; Claesson, P. M.; Attard, P. Bubbles, Cavities and the Long-Ranged Attraction between Hydrophobic Surfaces. *J. Phys. Chem.* **1994**, *98*, 8468–8480.
- (2) Seddon, J. R. T.; Lohse, D. Nanobubbles and Micropancakes: Gaseous Domains on Immersed Substrates. *J. Phys. Condens. Matter* **2011**, *23*, 133001.
- (3) Hampton, M. A.; Nguyen, A. V. Nanobubbles and the Nanobubble Bridging Capillary Force. *Adv. Colloid Interface Sci.* **2010**, *154*, 30–55.
- (4) Ishida, N.; Inoue, T.; Miyahara, M.; Higashitani, K. Nano Bubbles on a Hydrophobic Surface in Water Observed by Tapping-Mode Atomic Force Microscopy. *Langmuir* **2000**, *16*, 6377–6380.
- (5) Lou, S.-T.; Ouyang, Z.-Q.; Zhang, Y.; Li, X.-J.; Hu, J.; Li, M.-Q.; Yang, F.-J. Nanobubbles on Solid Surface Imaged by Atomic Force Microscopy. *J. Vac. Sci. Technol., B* **2000**, *18*, 2573–2575.
- (6) Zhang, X. H. Quartz Crystal Microbalance Study of the Interfacial Nanobubbles. *Phys. Chem. Chem. Phys.* **2008**, *10*, 6842–6848.
- (7) Zhang, X.; Chan, D. Y. C.; Wang, D.; Maeda, N. Stability of Interfacial Nanobubbles. *Langmuir* **2013**, *29*, 1017–1023.
- (8) Ljunggren, S.; Eriksson, J. C. The lifetime of a Colloid-Sized Gas Bubble in Water and the Cause of the Hydrophobic Attraction. *Colloids Surf., A* **1997**, *130*, 151–155.
- (9) Attard, P. Nanobubbles and the Hydrophobic Attraction. *Adv. Colloid Interface Sci.* **2003**, *104*, 75–91.
- (10) Zhang, X. H.; Quinn, A.; Ducker, W. A. Nanobubbles at the Interface between Water and a Hydrophobic Solid. *Langmuir* **2008**, *24*, 4756–4764.
- (11) Ducker, W. A. Contact Angle and Stability of Interfacial Nanobubbles. *Langmuir* **2009**, *25*, 8907–8910.
- (12) Wang, S.; Liu, M.; Dong, Y. Understanding the Stability of Surface Nanobubbles. *J. Phys.: Condens. Matter* **2013**, *25*, 184007.
- (13) Zhang, X.; Uddin, M. H.; Yang, H.; Toikka, G.; Ducker, W.; Maeda, N. Effects of Surfactants on the Formation and the Stability of Interfacial Nanobubbles. *Langmuir* **2012**, *28*, 10471–10477.
- (14) Brenner, M. P.; Lohse, D. Dynamic Equilibrium Mechanism for Surface Nanobubble Stabilization. *Phys. Rev. Lett.* **2008**, *101*, 214505.
- (15) Seddon, J. R. T.; Zandvliet, H. J. W.; Lohse, D. Knudsen Gas Provides Nanobubble Stability. *Phys. Rev. Lett.* **2011**, *107*, 116101.
- (16) Weijs, J. H.; Lohse, D. Why Surface Nanobubbles Live for Hours. *Phys. Rev. Lett.* **2013**, *110*, 054501.
- (17) Yang, S.; Dammer, S. M.; Bremond, N.; Zandvliet, H. J. W.; Kooij, E. S.; Lohse, D. Characterization of Nanobubbles on Hydrophobic Surfaces in Water. *Langmuir* **2007**, *23*, 7072–7077.
- (18) Guan, M.; Guo, W.; Gao, L.; Tang, Y.; Hu, J.; Dong, Y. Investigation on the Temperature Difference Method for Producing Nanobubbles and Their Physical Properties. *ChemPhysChem* **2012**, *13*, 2115–2118.
- (19) Berkelaar, R. P.; Seddon, J. R. T.; Zandvliet, H. J. W.; Lohse, D. Temperature Dependence of Surface Nanobubbles. *ChemPhysChem* **2012**, *13*, 2113–2117.
- (20) van Limbeek, M. A. J.; Seddon, J. R. T. Surface Nanobubbles As a Function of Gas Type. *Langmuir* **2011**, *27*, 8694–8699.
- (21) Tyrrell, J. W. G.; Attard, P. Images of Nanobubbles on Hydrophobic Surfaces and Their Interactions. *Phys. Rev. Lett.* **2001**, *87*, 176104.
- (22) Holmberg, M.; Kühle, A.; Garnaes, J.; Mørch, K. A.; Boisen, a. Nanobubble Trouble on Gold Surfaces. *Langmuir* **2003**, *19*, 10510–10513.
- (23) Agrawal, A.; Park, J.; Ryu, D. Y.; Hammond, P. T.; Russell, T. P.; McKinley, G. H. Controlling the Location and Spatial Extent of Nanobubbles Using Hydrophobically Nanopatterned Surfaces. *Nano Lett.* **2005**, *5*, 1751–1756.
- (24) Wang, Y.; Bhushan, B.; Zhao, X. Nanoindents Produced by Nanobubbles on Ultrathin Polystyrene Films in Water. *Nanotechnology* **2009**, *20*, 045301.
- (25) Zhang, X. H.; Maeda, N.; Craig, V. S. J. Physical Properties of Nanobubbles on Hydrophobic Surface in Water and Aqueous Solutions. *Langmuir* **2006**, *22*, 5025–5035.
- (26) Mazumder, M.; Bhushan, B. Propensity and Geometrical Distribution of Surface Nanobubbles: Effect of Electrolyte, Roughness, pH, and Substrate Bias. *Soft Matter* **2011**, *7*, 9184–9196.

- (27) Wu, Z. H.; Zhang, X. H.; Zhang, X. D.; Sun, J. L.; Dong, Y. M.; Hu, J. In situ AFM Observation of BSA Adsorption on HOPG with Nanobubble. *Chin. Sci. Bull.* **2007**, *14*, 1913–1919.
- (28) Wu, Z.; Chen, H.; Dong, Y.; Mao, H.; Sun, J.; Chen, S.; Craig, V. S. J.; Hu, J. Cleaning Using Nanobubbles: Defouling by Electrochemical Generation of Bubbles. *J. Colloid Interface Sci.* **2008**, *328*, 10–14.
- (29) Tarábková, H.; Janda, P. Nanobubble Assisted Nanopatterning Utilized for Ex Situ Identification of Nanobubbles. *J. Phys.: Condens. Matter* **2013**, *25*, 184001.
- (30) Kramer, J.; Tegenkamp, C.; Pfür, H. The Growth of NaCl on Flat and Stepped Silver Surfaces. *J. Phys.: Condens. Matter* **2003**, *15*, 6473–6483.
- (31) Sear, R. P. Nucleation: Theory and Applications to Protein Solutions and Colloidal Suspensions. *J. Phys.: Condens. Matter* **2007**, *19*, 033101.
- (32) Anwar, J.; Zahn, D. Uncovering Molecular Processes in Crystal Nucleation and Growth by Using Molecular Simulation. *Angew. Chem., Int. Ed.* **2011**, *50*, 1996–2013.
- (33) Kameda, N.; Sogoshi, N.; Nakabayashi, S. Nitrogen Nanobubbles and Butane Nanodroplets at Si(100). *Surf. Sci.* **2008**, *602*, 1579–1584.
- (34) Zhang, X. H.; Zhang, X.; Sun, J.; Zhang, Z.; Li, G.; Fang, H.; Xiao, X.; Zeng, X.; Hu, J. Detection of Novel Gaseous States at the Highly Oriented Pyrolytic Graphite–Water Interface. *Langmuir* **2007**, *23*, 1778–1783.
- (35) Zhang, L.; Zhang, X.; Fan, C.; Zhang, Y.; Hu, J. Nanoscale Multiple Gaseous Layers on a Hydrophobic Surface. *Langmuir* **2009**, *25*, 8860–8864.
- (36) Seddon, J. R. T.; Bliznyuk, O.; Kooij, E. S.; Poelsema, B.; Zandvliet, H. J. W.; Lohse, D. Dynamic Dewetting through Micropancake Growth. *Langmuir* **2010**, *26*, 9640–9644.
- (37) Peng, H.; Hampton, M. A.; Nguyen, A. V. Nanobubbles Do Not Sit Alone at the Solid–Liquid Interface. *Langmuir* **2013**, *29*, 6123–6130.
- (38) Yang, C. W.; Lu, Y. H.; Hwang, I. S. Condensation of Dissolved Gas Molecules at a Hydrophobic/Water Interface. *Chin. J. Phys.* **2013**, *51*, 174–186.
- (39) Walczyk, W.; Schön, P. M.; Schönherr, H. The Effect of Peakforce Tapping Mode AFM Imaging on the Apparent Shape of Surface Nanobubbles. *J. Phys.: Condens. Matter* **2013**, *25*, 184005.
- (40) Borkent, B. M.; de Beer, S.; Mugele, F.; Lohse, D. On the Shape of Surface Nanobubbles. *Langmuir* **2010**, *26*, 260–268.
- (41) de Gennes, P. G. Wetting: Statics and Dynamics. *Rev. Mod. Phys.* **1985**, *57*, 827–863.
- (42) Py, C.; Reverdy, P.; Doppler, L.; Bico, J.; Roman, B.; Baroud, C. N. Capillary Origami: Spontaneous Wrapping of a Droplet with an Elastic Sheet. *Phys. Rev. Lett.* **2007**, *98*, 156103.
- (43) Huang, R.; Im, S. H. Dynamics of Wrinkle Growth and Coarsening in Stressed Thin Films. *Phys. Rev. E* **2006**, *74*, 026214.